

UC Davis

UC Davis Previously Published Works

Title

Periventricular microglial cells interact with dividing precursor cells in the nonhuman primate and rodent prenatal cerebral cortex

Permalink

<https://escholarship.org/uc/item/18m4j2q0>

Journal

The Journal of Comparative Neurology, 527(10)

ISSN

1550-7149

Authors

Noctor, Stephen C
Penna, Elisa
Shepherd, Hunter
et al.

Publication Date

2019-07-01



DOI

10.1002/cne.24604

Peer reviewed

RESEARCH ARTICLE

Periventricular microglial cells interact with dividing precursor cells in the nonhuman primate and rodent prenatal cerebral cortex

Stephen C. Noctor^{1,2}  | Elisa Penna² | Hunter Shepherd^{1,3} | Christian Chelson^{1,3} | Nicole Barger² | Verónica Martínez-Cerdeño^{1,4,5}  | Alice F. Tarantal^{6,7,8,9}

¹MIND Institute, School of Medicine, UC Davis, Sacramento, California

²Department of Psychiatry and Behavioral Sciences, School of Medicine, UC Davis, Sacramento, California

³Brigham Young University – Idaho, Rexburg, Idaho

⁴Department of Pathology and Laboratory Medicine, School of Medicine, UC Davis, Davis, California

⁵Institute for Pediatric Regenerative Medicine, Shriners Hospital, Sacramento, California

⁶Department of Pediatrics, School of Medicine, UC Davis, Davis, California

⁷Department of Cell Biology and Human Anatomy, School of Medicine, UC Davis, Davis, California

⁸Center for Fetal Monkey Gene Transfer for Heart, Lung, and Blood Diseases, UC Davis, Davis, California

⁹California National Primate Research Center, UC Davis, Davis, California

Correspondence

Stephen C. Noctor, 2805 50th Street; Sacramento, California, 95817.
Email: scnoctor@ucdavis.edu

Funding information

National Institute of Mental Health, Grant/Award Number: MH101188; National Heart, Lung, and Blood Institute, Grant/Award Number: HL085794; NIH Intellectual and Developmental Disabilities Research Center, Grant/Award Number: U54 HD079125; UC Davis School Medicine Department of Psychiatry and Behavioral Sciences; California National Primate Research Center, Grant/Award Number: OD011107

Abstract

Cortical proliferative zones have been studied for over 100 years, yet recent data have revealed that microglial cells constitute a sizeable proportion of ventricular zone cells during late stages of cortical neurogenesis. Microglia begin colonizing the forebrain after neural tube closure and during later stages of neurogenesis populate regions of the developing cortex that include the proliferative zones. We previously showed that microglia regulate the production of cortical cells by phagocytosing neural precursor cells (NPCs), but how microglia interact with NPCs remains poorly understood. Here we report on a distinct subset of microglial cells, which we term periventricular microglia, that are located near the lateral ventricle in the prenatal neocortex. Periventricular microglia exhibit a set of similar characteristics in embryonic rat and fetal rhesus monkey cortex. In both species, these cells occupy ~60 μm of the ventricular zone in the tangential axis and make contact with the soma and processes of NPCs dividing at the ventricle for over 50 μm along the radial axis. Periventricular microglia exhibit notable differences across species, including distinct morphological features such as terminal bouton-like structures that contact mitotic NPCs in the fetal rhesus monkey but not in rat. These morphological distinctions suggest differential functions of periventricular microglia in rat and rhesus monkey, yet are consistent with the concept that microglia regulate NPC function in the developing cerebral cortex of mammalian species.

KEYWORDS

cerebral cortex, fetal development, neural precursor cells, nonhuman primate, periventricular microglial cells, prenatal, radial glial cells, ventricular zone, RRID: AB_592962, RRID: AB_839504, RRID: AB_2224402

1 | INTRODUCTION

Precursor cells in the developing cerebral cortex were identified near the surface of the lateral ventricle over 100 years ago (see His, 1889). Since that time, the morphology, distribution, and function of precursor cells, and the cellular composition of the proliferative zones in the developing neocortex have been a central focus of investigation. Our understanding of the principal characteristics of neural precursor cells (NPCs) was originally derived from analysis of nervous tissue staining techniques such as Golgi whole-cell labeling. New insight emerged through technical advances that included electron microscopy, immunohistochemistry, electrophysiology combined with whole-cell labeling, reporter gene whole-cell labeling, and reporter expression linked to specific genes. While major advances have been achieved from the application of new technologies specific to research on the developing brain, our understanding of basic fundamentals of forebrain development, such as cellular composition and cell-cell interactions in the proliferative zones, remains incomplete.

Microglial cells are the resident innate immune cells of the central nervous system (Wolf, Boddeke, & Kettenmann, 2017). Microglia are derived from the yolk sac in mouse (Alliot, Godin, & Pessac, 1999; Ginhoux et al., 2010), begin to colonize the murine cerebral cortex by embryonic day (E) 11.5 (Arno et al., 2014; Swinnen et al., 2013), in rat by E13 (Cunningham, Martinez-Cerdeño, & Noctor, 2013b), in rhesus monkey during the first trimester (prior to 50 days gestation) (Cunningham et al., 2013b), and in the human cerebrum by 6 weeks of gestation (Andjelkovic, Nikolic, Pachter, & Zecevic, 1998; Verney, Monier, Fallet-Bianco, & Gressens, 2010). In each species, microglia initially colonize specific regions and laminae of the developing brain that include the cortical proliferative zones (Cunningham et al., 2013b). Microglia participate in developmental programs that include the establishment of axonal pathways (Squarzoni et al., 2014), synapse development and maintenance (Paolicelli et al., 2011; Salter & Stevens, 2017; Schafer et al., 2012), and cortical layer formation (Squarzoni et al., 2014; Ueno et al., 2013). Using antibodies against the precursor cell-specific transcription factors Pax6 and Tbr2, and against microglial cells, we previously showed that microglia contact, envelope, and phagocytose NPC nuclei in the normally developing prenatal cerebral cortex (Cunningham et al., 2013b). To better understand intercellular relationships in the cortical proliferative zones, we next labeled precursor cells and microglia with the enhanced green fluorescent protein (eGFP) via in utero lentiviral vector-mediated intraventricular injections in early gestation fetal rhesus monkeys. This approach revealed numerous contacts between microglia and radial glial cells, radial glial fibers, and intermediate progenitor cells throughout the ventricular zone (VZ) and subventricular zone (SVZ) in the rhesus monkey (Barger et al., 2018). These data also provided evidence of a previously undescribed population of microglial cells that we termed “periventricular microglia”. These microglia are located within the VZ near the ventricle, and contact mitotic NPCs undergoing division at the surface of the ventricle in the embryonic rat and fetal rhesus monkey telencephalon (Barger et al., 2018). This microglial subtype had not previously been identified or investigated with respect to cortical neurogenesis.

The present study investigates the cellular composition and intercellular relationships in the prenatal cortical proliferative zones with respect to periventricular microglia in embryonic rat and the fetal rhesus monkey. Here, we further characterize periventricular microglia and quantify contact points between microglia and actively dividing NPCs in prenatal rat and fetal rhesus monkey at the same stage of cortical neurogenesis. These studies revealed abundant contacts between periventricular microglia and mitotic NPCs, demonstrating that microglia are an integral component of the prenatal cortical proliferative zones, which are consistent with the concept that microglia impact cortical development.

2 | MATERIAL AND METHODS

2.1 | Animals

All animal procedures conformed to the requirements of the Animal Welfare Act and protocols were approved prior to implementation by the Institutional Animal Care and Use Committee at the University of California, Davis.

Embryonic day (E)19 rat embryos were transcardially perfused with 0.1 M phosphate buffered saline (PBS) followed by 4% paraformaldehyde in PBS (PFA). Brains were extracted and post-fixed in 4% PFA for 24 hr, washed in PBS and stored in PBS with 0.01% sodium azide at 4°C. Cortical slab preparations were prepared from three embryos by excising the dorsal portion of the cerebral cortex from each hemisphere using micro-scissors and an Olympus SZ61 dissecting scope (Figure 1a).

Cortical slab preparations are blocks of tissue that encompass the full thickness of the developing cerebral cortex from the ventricle to the meningeal surface. The slab explants minimize cut surfaces that intersect cell bodies, cell processes, intercellular connections, and relationships between adjacent cells. We previously used the cortical slab approach to identify the morphology and physiological profile of radial glial cells in live culture preparations (Noctor et al., 2002).

Normally cycling, adult female rhesus monkeys (*Macaca mulatta*) with a history of prior pregnancy were bred and identified as pregnant using established methods (Tarantal, 2005) ($N = 2$). Pregnancy in the rhesus monkey is divided into trimesters by 55-day increments with 0–55 days gestation representing the first trimester, 56–110 days gestation representing the second trimester, and 111–165 days gestation the third trimester (term 165 ± 10 days). All fetuses were assessed sonographically to confirm normal growth and development until fetal tissue harvest at 90 days gestation (second trimester) according to standardized protocols (Tarantal et al., 1998). Tissues were transcardially perfused and immersed in 4% PFA for 2–3 days. The right hemisphere was cryoprotected in 30% sucrose and tissue was cryosectioned at 100 μm on a sliding microtome.

2.2 | Embryonic rat immunohistochemistry

Antigen retrieval was performed by heating free-floating slabs in 10 mM Citrate Buffer (pH 6.0) containing 10 mM Citric Acid (Fisher) and (v/v) 0.5% Tween-20 (Acros) at 85°C for 25 min and then allowing to cool to room temperature (RT) for 35 min. Slabs were rinsed

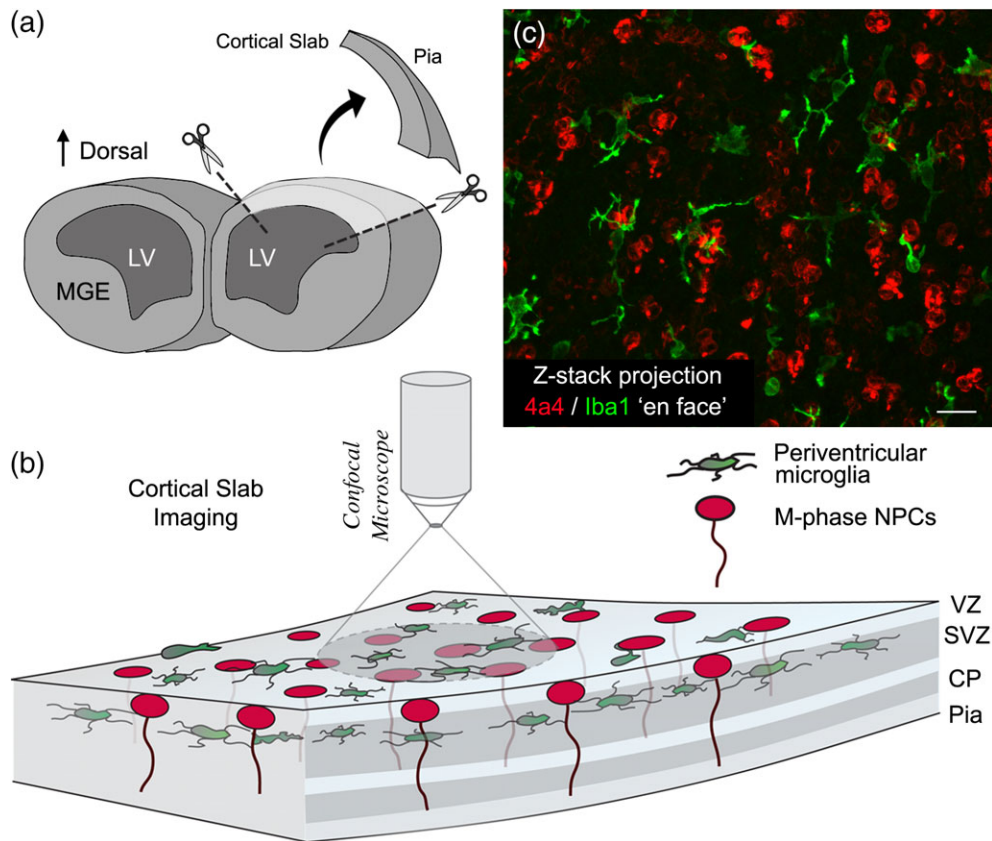


FIGURE 1 Preparation of cortical slabs. (a) The dorsal cortex was excised from perfused brains obtained from E19 rats. Excised blocks of cortical tissue encompassed the full thickness of cortex from the ventricle to the pial surface and extended ~1.5 mm in the medio-lateral axis and 2.0 mm in the rostro-caudal axis. (b) Slabs were immunostained with antibodies to label M-phase NPCs (4A4, red) and periventricular microglia (Iba1, green), and imaged on a confocal microscope with the ventricular surface facing the objective. (c) Projection image of a 100 μm thick Z-stack obtained from an E19 rat cortical slab showing Iba1⁺ periventricular microglia (green) and 4A4⁺ NPCs (red) dividing at the ventricular surface. Ninety-two percent of periventricular microglia contacted mitotic NPCs. Scale bar in c = 20 μm [Color figure can be viewed at wileyonlinelibrary.com]

three times for 10 min each in PBS and then blocked in blocking buffer solution containing (v/v) 10% fetal donkey serum, 0.1% Triton X-100 (Acros), and (w/v) 0.2% gelatin (Acros) for 2 hr at RT. Slabs were rinsed once for 5 min in PBS and incubated in the primary antibody buffer composed of (v/v) 2% fetal donkey serum, 0.02% Triton X-100, and (w/v) 0.04% gelatin containing primary antibodies (mouse antiphosphorylated vimentin 4A4, 1:100, MBL: Cat# DO76-3S, clone 4A4, RRID: AB_592962) and rabbit anti-Iba1 (1:150 Wako: Cat# O19-19,741, RRID: AB_839504), for 3 days at 4°C on a rocking platform. Slabs were rinsed 5 \times 10 min in PBS, then incubated for 4.5 hr in secondary antibody buffer composed of (v/v) 2% fetal donkey serum, and 0.02% Triton X-100, (w/v) 0.04% gelatin containing donkey antimouse and donkey antirabbit secondary antibodies conjugated to Cy2/Dylight 488, and Cy5/Dylight 649 (1:250 Jackson Laboratories) at RT. Slabs were placed in DAPI (1:1,000, Sigma) for 10 min and rinsed five times for 10 min. Slabs were imaged in concave glass well plates immersed in PBS, with the ventricular surface facing the objective, on an Olympus Fluoview 1,000 confocal microscope. See Table 1.

2.3 | Fetal rhesus monkey immunohistochemistry

Tissue was mounted on SuperFrost slides (Fisher), submerged in 10 mM Citrate Buffer (Fisher), pH 6, and heated in a steamer for

15 min (modification of Tang, Falls, Li, Lane, & Luskin, 2007). After citrate buffer reached RT, tissue was rinsed three times for 5 min and incubated in blocking buffer containing 10% donkey serum (Millipore) and 1% Triton X-100 (Acros) for 1.5 hr at RT. Tissue was incubated for 2–3 days in a primary antibody buffer containing 2% donkey serum, 1% Triton X-100, and antibodies including mouse antiphosphorylated vimentin (4A4, 1:100; MBL, Cat# DO76-3S, clone 4A4, RRID: AB_592962) and goat anti-Iba1 (1:200, Abcam, Cat# ab5076, RRID: AB_2224402). Tissue was rinsed and incubated for 2 hr at RT in a secondary antibody buffer with 2% donkey serum and 1% Triton X-100 that included donkey anti-mouse and donkey anti-goat conjugated to the fluorophores AF488 and AF647 at a concentration of 1:250 (Jackson ImmunoResearch). After secondary incubation tissue was rinsed in two times 5 min in PBS, stained with DAPI (Sigma, 1:1000) in PBS for 15 minutes followed by 2 \times PBS washes, and then coverslipped with Mowiol. See Table 1.

2.4 | Imaging and analysis

Cortical slabs were imaged on an Olympus Fluoview 1000 confocal microscope from the surface to a depth of 70–100 μm from the ventricular surface (Figure 1). Image stacks were acquired at 1.0 μm steps using or 60 \times (NA, 1.4) or 40 \times (NA 0.7) objectives. Iba1⁺ microglial cells and all of their processes were captured in their entirety in the Z-

TABLE 1 Table of primary antibodies used

Antigen	Description of immunogen	Source, host species, cat. #, clone or lot#, RRID	Concentration used
Phosphorylated vimentin (ser 55)	Synthetic MPV55 phosphopeptide corresponding to mouse phosphorylated vimentin Ser55 (SLYSS-phosphoS55-PGGAYC-KLH)	MBL, mouse monoclonal, cat# DO76-3S, clone 4A4, RRID: AB_592962	1:100
Iba1, a calcium-binding protein with a molecular weight of 17,000 specifically expressed in macrophage/microglia	Synthetic peptide corresponding to C-terminus of Iba1	Wako, rabbit polyclonal, cat# 019-19,741, RRID: AB_839504	1:150
Iba1, a calcium-binding protein with a molecular weight of 17,000 specifically expressed in macrophage/microglia	Synthetic peptide corresponding to human Iba1 aa 135-147 (C terminal). Accession number(s): NP_116573.1; NP_001614.3 Sequence: C-TGPPAKKAISELP	Abcam, goat polyclonal, cat# ab5076, RRID: AB_2224402	1:200

stacks. Each periventricular microglial cell captured in these images was included for analysis (rat, $n = 129$ cells; monkey, $n = 27$ cells). For each periventricular microglial cell we measured the diameter of the soma, the number of principal processes emerging from the soma, and the distance of the soma from the ventricular surface. We quantified the number of contact points between the microglia and 4A4⁺ NPCs, recording whether contact occurred on the NPC soma or pial process. Contact was defined as two cell bodies/cell processes whose external surfaces touch each other—in this case Iba1⁺ soma or processes that were directly adjacent to 4A4⁺ cell bodies and/or pial processes—and recorded the cell cycle stage of the 4A4⁺ cells (prometaphase, metaphase, anaphase, or telophase).

2.5 | Statistics

Data are reported as mean \pm S.D. We performed *t*-tests with a two-tailed *p*-value nonparametric test to statistically compare the number of cells positive for specific markers, and the cells' characteristic tests scores between groups using GraphPad Prism (GraphPad Software, Inc.).

3 | RESULTS

Our previously published studies revealed a population of microglial cells located in the VZ that was positioned close to the lateral ventricle in embryonic rat and fetal rhesus monkey cerebral cortex, which we termed periventricular microglia (Barger et al., 2018). In coronal sections we noted that periventricular microglia contacted radial glial cells, and radial glial cell processes in the proliferative zones (Barger et al., 2018). However, viewing periventricular microglia in coronal sections did not fully capture the three-dimensional (3D) morphology of these cells, nor did it fully capture the intercellular relationships between microglia and NPCs. Coronal or sagittal sections of the prenatal brain can often transect cellular processes that extend in multiple directions. Maintaining long cellular processes in an explant of brain tissue improves analysis of intercellular interactions and contacts. This is particularly true for cell types such as radial glial cells, which have long pial processes that extend hundreds of microns from the cell body.

We used an alternative approach and examined intercellular relationships between microglia and NPCs in cortical slab preparations.

Cortical slabs are blocks of tissue excised from the cerebral cortex that encompass the full thickness of the developing cortex from the ventricle to the pial surface. Our embryonic rat explants extended ~ 1.5 mm in the medio-lateral axis and up to 2.0 mm in the rostro-caudal axis (Figure 1). Cortical slab explants minimize the cut surfaces that intersect cell bodies and cellular processes and maximize retention of the intercellular relationships and connections between adjacent cells. The cortical slab preparations did not include the ganglionic eminence or the medial wall of the cortex. We previously used cortical slabs from embryonic rat to examine the physiological profile and morphology of radial glial cells in live explants (Noctor et al., 2002). For the present study cortical slabs of the dorsal cortex were excised from perfused E19 rat cortices. Mitotic NPCs were labeled with antibodies against phosphorylated vimentin (4A4) to label M-phase cells (Cunningham, Martinez-Cerdeño, & Noctor, 2013a; Kamei et al., 1998; Noctor et al., 2002), microglial cells were labeled with anti-Iba1 (Barger et al., 2018; Cunningham et al., 2013b; Imai, Iba, Ito, Ohsawa, & Kohsaka, 1996), and slabs were imaged on a confocal microscope (Figure 1). We analyzed the morphology of individual Iba1⁺ periventricular microglia and the contacts between microglia and 4A4⁺ cells in the slab preparations. Contact was defined as in the Oxford English Dictionary: "mutual relation of two bodies whose external surfaces touch each other" and was determined through analysis of sequential optical plane images within Z-stacks encompassing up to 100 μm in the radial dimension from the ventricle through the VZ. Contact between these two cell types often entailed extensive apposition between soma and/or processes of Iba1⁺ and 4A4⁺ cells that extended over 10 μm , but in some cases the contact was more discrete and consisted of two processes that abutted one another.

3.1 | Rat periventricular microglia make extensive contacts with mitotic NPCs

The somata of Iba1⁺ periventricular microglia in the embryonic rat neocortex averaged 10.77 ± 2.10 μm in diameter, and the maximum diameter of the cells and all of their processes was ~ 60 μm in the radial and tangential dimensions. The somata of periventricular microglia were positioned at an average distance of $31.02 \pm 12.20^{\text{STD}}$ μm from the ventricle (range 2–60 μm), most often superficial to the population of NPCs that divide at the ventricular surface. In embryonic rat the periventricular microglia typically extended three main processes

from the soma (Figure 2a). The principal processes generally branched two or three times and extended at least one thin process toward the ventricle.

In the E19 rat periventricular microglia made extensive, close contact with mitotic 4A4⁺ NPCs. Each periventricular microglia made, on average, $3.41 \pm 2.60^{\text{STD}}$ contacts with mitotic NPCs (range 0–15 contacts, $n = 129$ microglia). Our data set included 12 periventricular microglia that had an amoeboid shape, lacked processes, and did not contact 4A4⁺ cells. Excluding amoeboid microglia from analysis increased the number of NPC contacts per microglia to a value of $3.66 \pm 2.60^{\text{STD}}$. Most microglia contacted the same NPC more than once on the pial process and/or soma. As a result, the number of unique NPCs that each microglia contacted averaged $2.84 \pm 1.80^{\text{STD}}$.

Thus, each periventricular microglia simultaneously contacted about three mitotic NPCs dividing at the ventricle of the E19 rat neocortex. Among periventricular microglia we analyzed ($n = 129$), ~9% did not contact an NPC; 13% contacted one NPC; 17% contacted two NPCs; 17% contacted three; and 44% contacted more than three NPCs.

We quantified the proportion of periventricular microglia that contacted either the pial process, the soma, or both of dividing NPCs. We found that 63% of the periventricular microglia contacted only the pial process of 4A4⁺ mitotic NPCs, 28% contacted only the soma, and 9% contacted both soma and the pial process of 4A4⁺ mitotic NPCs. Thus, 37% of the periventricular microglia made contact with the soma of a precursor cell dividing at the ventricle. We next focused on periventricular microglial cells that contacted the soma of mitotic

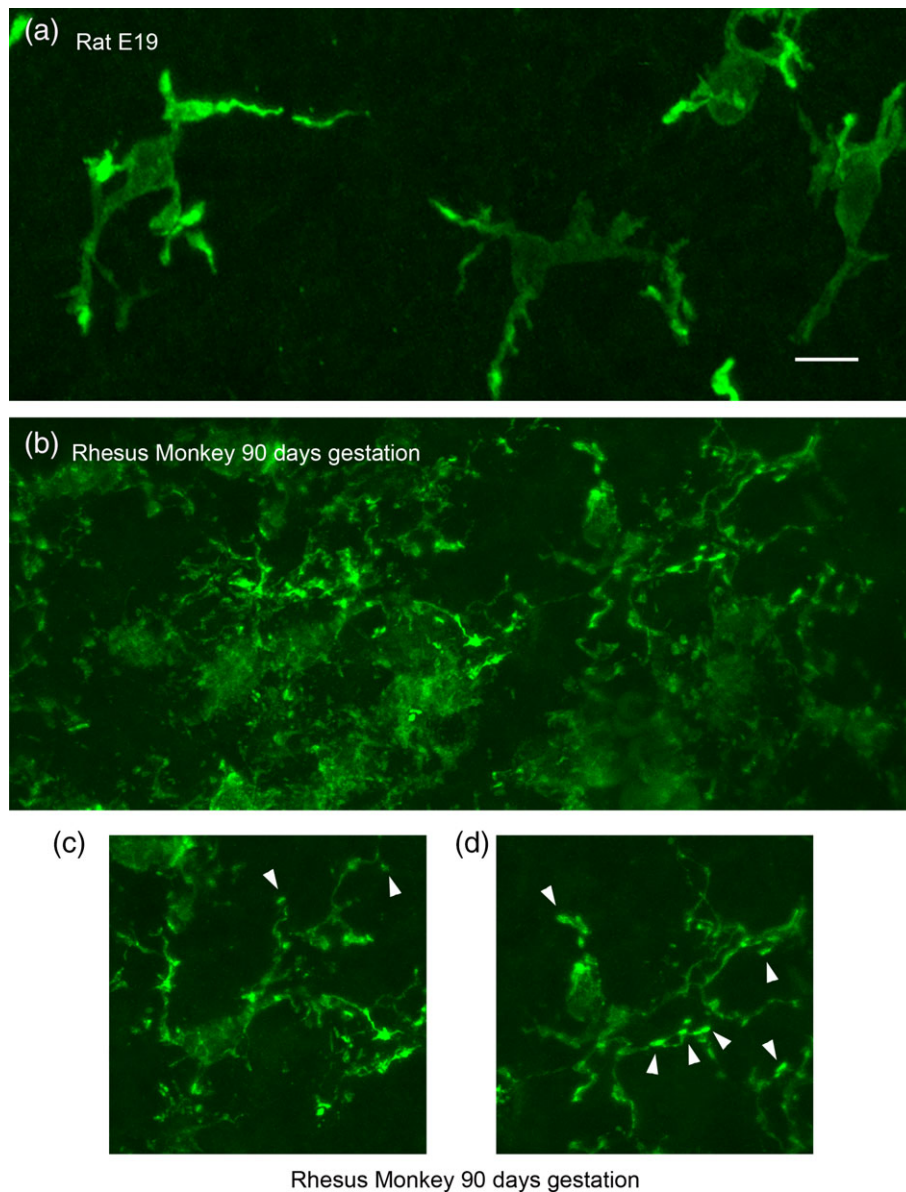


FIGURE 2 Morphology of periventricular microglia in E19 rat and 90 days gestation (second trimester) fetal rhesus monkey. (a) Projection images of periventricular microglia stained with Iba1 (green) in the E19 rat cortical ventricular zone. These cells usually extended three or four principal processes and occupied ~60 μm in X, Y, and Z planes. (b) The density of microglial cells near the surface of the ventricle was much higher in the fetal rhesus monkey. (c, d) Periventricular microglia in second trimester rhesus monkey also extended three or four principal processes, but the processes were more ramified and often terminated with Bouton-like structures that were adjacent to mitotic soma (arrowheads). Scale bar in a = 10 μm and applies to all panels [Color figure can be viewed at wileyonlinelibrary.com]

NPCs to further characterize this subset of contacts. 4A4 immunostaining permits straightforward identification of the prophase, metaphase, anaphase, and telophase stages of mitosis (Weissman, Noctor, Clinton, Honig, & Kriegstein, 2003). The subset of periventricular microglia that contacted the soma of mitotic NPCs was closer to the ventricle, averaging 25.0 μm versus 31.0 μm for all periventricular microglia. We observed that periventricular microglia were more likely to contact NPCs undergoing cytokinesis: 83% contacted a precursor cell that was in telophase when nascent daughter cells take form as the NPC completes cell division.

Periventricular microglia in the embryonic rat cortex occupied a territory that extended $\sim 60 \mu\text{m}$ in the tangential and radial dimensions. Microglial somata were positioned $\sim 30 \mu\text{m}$ from the ventricle as noted above, and these cells extended processes both toward the ventricle and away from the ventricle. As a consequence, individual periventricular microglial cells often contacted the soma of mitotic NPCs at the ventricle, and the pial fiber emanating from that NPC as the fiber coursed radially through the VZ. Figure 3 presents a series of single optical planes from a confocal Z-stack to highlight the morphology and intercellular relationships of periventricular microglia. The images show the 3D morphology of a single periventricular microglial cell (Iba1⁺, green), the position of the microglial soma with reference to the ventricle (Figure 3, asterisk in 18–24 μm panels), the extension of processes both toward the ventricle and $\sim 60 \mu\text{m}$ away from the ventricle, and the intercellular contacts between this microglial cell and mitotic NPCs at the ventricle (4A4⁺, red). The somata of mitotic NPCs are numbered (1, 2, 3), and the pial fiber emanating from each cell is identified with the same number. The pial fiber from cells 1 and 2 were traced through all optical planes in the Z-stack, and the pial fiber of cell 3 was traced $\sim 20 \mu\text{m}$ from the ventricle. The thickness of the 4A4⁺ pial fibers alternated between portions that were very thin ($< 0.5 \mu\text{m}$) and much thicker (up to 4 μm), reflecting the presence of varicosities along the pial fibers of M-phase NPCs (Barger et al., 2018; Noctor, Martínez-Cerdeño, Ivic, & Kriegstein, 2004; Noctor, Martínez-Cerdeño, & Kriegstein, 2008).

We observed repeated contacts between a periventricular microglial cell and single pial fibers as shown in Figure 3. For example, the pial fiber emanating from Cell 1 was contacted by the microglia cell from 14 to 20 μm from the ventricle, and again from 42 to 50 μm from the ventricle (Figure 3, and Supporting Information Movie 1). The periventricular microglia likely contacted other cells and pial fibers emanating from NPCs that were not labeled with the 4A4 antibody.

The morphology of contact points between periventricular microglia and NPCs in the E19 rat varied as we previously reported in a study on the fetal rhesus monkey cortex (Barger et al., 2018). In the E19 rat, periventricular microglia often extended processes that terminated on the soma and/or pial process of mitotic 4A4⁺ cells. In many cases the microglial processes ran parallel with pial processes and maintained contact over a span of 5–10 μm (e.g., Figures 3, 14–20 μm panels). While the intercellular contacts often appeared to consist of a microglial process extension that made contact with a mitotic NPC, we also noted extensions from the pial process that contacted periventricular microglia (Figure 3, white arrowhead 24–26 μm panels, Supporting Information Movie 1). Figure 4 illustrates the relative

positions and intercellular relationships between periventricular microglia and mitotic NPCs.

We noted that in some cases the processes of periventricular microglia appeared to travel through the soma of 4A4⁺ cells dividing at the surface. These Iba1⁺ processes were visibly present in confocal optical planes that transected the soma of 4A4⁺ NPCs (Figure 5). These data suggest that the outer membrane of mitotic NPCs is not a simple sphere, but instead the 4A4⁺ cells must have a complex outer membrane that includes grooves or channels through which the processes of periventricular microglia course.

3.2 | Morphology and intercellular contacts of rhesus monkey periventricular microglia

We next performed a qualitative analysis of the morphology and characteristics of periventricular microglia in tissue prepared from the occipital lobe of 90 days gestation (second trimester) fetal rhesus monkey, which represents the same relative stage of cortical neurogenesis as the E19 rat (Bayer & Altman, 1991; Rakic, 1974). Periventricular microglia in the rhesus monkey shared basic features with those in the rat. The diameter of periventricular microglial somata in the monkey was similar to those in the rat (10.08 \pm 1.1 μm vs. 10.77 in rat), and the cells occupied a volume of $\sim 60 \mu\text{m}$ in the tangential and radial dimensions similar to the rat. Rat and monkey periventricular microglia typically elaborated three principal processes. However, periventricular microglia in the rhesus monkey were significantly closer to the ventricle than in the rat: 14.8 \pm 8.6^{STD} μm versus 31.02 \pm 12.2^{STD} μm ($p < .0001$, Figure 6). We also noted that the density of periventricular microglia was higher in rhesus monkey than in rat as we have previously reported (Figure 2a,b, (Barger et al., 2018)). To account for potential differences in cellular density in the rat and rhesus monkey periventricular proliferative zone we quantified the number of microglia in relation to the total number of DAPI⁺ cells in 100 $\mu\text{m} \times 100 \mu\text{m}$ bins. We found that in the E19 rat periventricular microglia constituted 1.21 \pm 0.75% of all cells close to the ventricle ($n = 571$ cells, three fetuses), while in the gestation day 90 fetal monkey microglia constituted 5.94% of all cells near the ventricle ($n = 344$ cells, two fetuses), demonstrating that periventricular microglia constitute a higher proportion of ventricular cells in the nonhuman primate. We also noted that the morphology of periventricular microglial cells in the fetal rhesus monkey was much more complex than in rat. Periventricular microglia in rhesus monkey had more secondary and tertiary branches and extended thin processes that terminated with bouton-like structures, which we did not observe in the E19 rat (Figure 2c,d).

In addition, we noted that periventricular microglia in the fetal rhesus monkey extended large membranous sheets that surrounded and enveloped neighboring cells, including Tbr2⁺ NPCs. As a result of the density of microglial cells in the rhesus monkey, in some regions of the proliferative zones the membranous extensions were nearly continuous with processes that extended from neighboring microglia. Figure 7 and Supporting Information Movie 2 show a series of sequential 1 μm step optical planes that highlight the complex 3D cytoarchitecture of periventricular microglia in the fetal rhesus monkey VZ. We have previously shown microglial phagocytosis of NPCs during late stages of

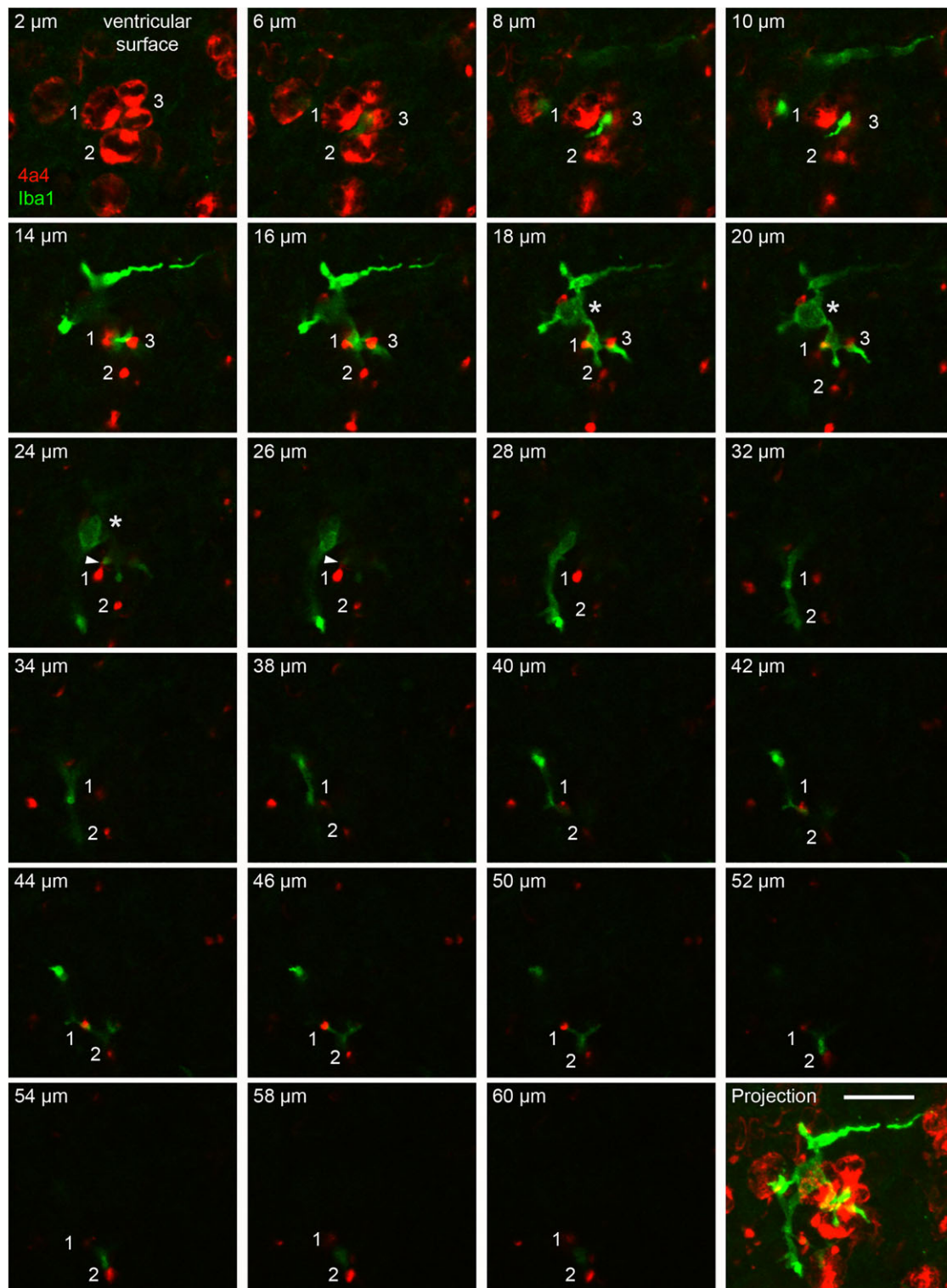


FIGURE 3 A single periventricular microglial cell (Iba1, green) in the E19 rat extended processes toward the ventricle where it contacted multiple mitotic NPCs (4A4, red), and extended additional process away from the ventricle that made contact with the pial fibers emanating from these NPCs over a distance of 60 μm from the ventricle. Panels show single optical plane images from a confocal Z-stack starting at 2 μm from the ventricle in the upper left and proceeding to 60 μm from the ventricle. The lower right panel shows the projected image of this Z-series. Three mitotic 4A4⁺ NPCs are numbered. The upper left panel shows the soma of these cells, two in metaphase (cells 1, 2), and one in telophase (3). The pial fiber of cell three is traceable for a distance of 20 μm from the ventricle. The pial fibers of cells 1 and 2 are visible throughout the Z-stack. The images from optical planes 18–24 μm show the soma of the cell (asterisk). The microglia extended a process toward the ventricle that contacted the surface membrane of cell 3. This process also coursed between and contacted the pial fibers of cells 1 and 3 (optical planes 14–20 μm). We also noted extensions from the pial process that contacted periventricular microglia (white arrowhead 24–26 μm panels). The microglial cell extended another process away from the ventricle and this process coursed between and contacted the pial processes of cells 1 and 2 (optical planes 42–54 μm) and was no longer visible at a distance of more than 60 μm from the ventricle. The scale bar at bottom right = 20 μm . The entire Z-stack can be viewed as a QuickTime movie in Supporting Information Movie 1 [Color figure can be viewed at wileyonlinelibrary.com]

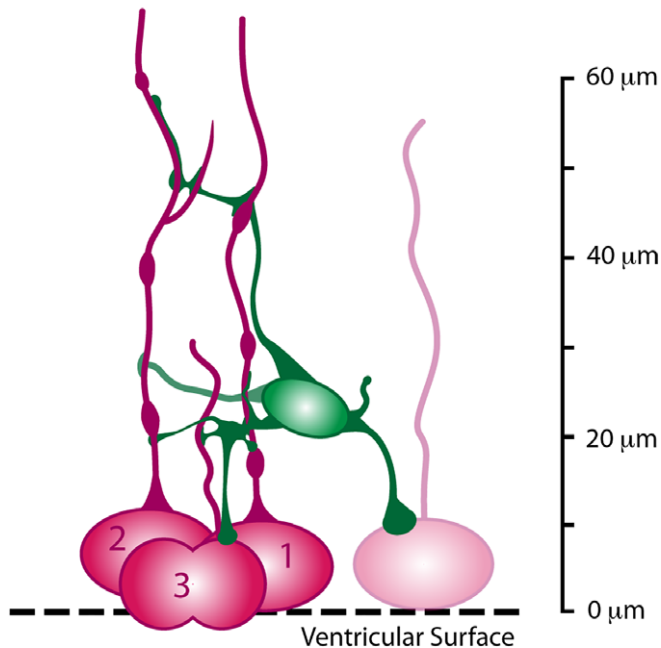
Periventricular Microglia
in the Embryonic Rat

FIGURE 4 Schematic drawing summarizing the position and intercellular connections between periventricular microglia and mitotic NPCs in the embryonic rat cerebral cortex. Individual periventricular microglia on average contact over 3 NPCs at the same time, and make multiple contacts with the soma and pial fiber of the same NPCs for up to 60 μm in the radial dimension [Color figure can be viewed at wileyonlinelibrary.com]

cortical neurogenesis in the monkey (Cunningham et al., 2013b). Figure 7 and Supporting Information Movie 2 show that in the 90 days gestation fetal rhesus monkey the membranous sheets of individual periventricular microglial cells entirely enveloped multiple NPCs. The microglial membranous extensions were uncommon in the embryonic rat neocortex.

We recorded fewer contacts between periventricular microglia and NPCs in the 90 days gestation fetal rhesus monkey compared to

the E19 rat. At this stage of development in rhesus monkey fewer NPC divisions occur at the ventricular surface compared to the same relative stage of cortical neurogenesis in the rat (Martinez-Cerdeño et al., 2012), because the vast majority of NPC divisions have shifted to the SVZ (Martinez-Cerdeño et al., 2012; Smart, Dehay, Giroud, Berland, & Kennedy, 2002). Thus, while the density of microglial cells was considerably higher in fetal rhesus monkey, the density of surface NPC divisions was lower. Consequently, the number of intercellular contacts between periventricular microglia and mitotic NPCs in the 90 days gestation rhesus monkey was lower ($1.69 \pm 1.2^{\text{STD}}$) than we observed in the E19 rat.

4 | DISCUSSION

Defining and understanding cellular composition in the cortical proliferative zones is crucial for understanding how NPCs produce the neurons and glial cells that populate mature neocortex. The data we present provide further evidence that microglial cells are an integral component of prenatal cortical proliferative zones, and contribute to the complex cellular matrix in which NPCs reside and function. We previously showed that microglial cells phagocytose NPCs in the prenatal cortex (Cunningham et al., 2013b), and make extensive contacts with the soma and processes of NPCs in the fetal monkey brain (Barger et al., 2018). Here we focused our analysis on a subset of microglial cells that are positioned in the VZ near the ventricle, which we have termed periventricular microglia. We analyzed intercellular relationships between periventricular microglia and actively dividing NPCs in cortical tissue obtained from naïve E19 rats and second trimester (90 days gestation) fetal rhesus monkeys. We labeled microglia with the Iba1 antibody (Cunningham et al., 2013b; Imai et al., 1996), and actively dividing NPCs with the M-phase marker 4A4 (Cunningham et al., 2013a; Kamei et al., 1998; Noctor et al., 2002). The 4A4 antibody has several key advantages that aid study of basic NPC characteristics. The 4A4 antibody labels the soma of mitotic NPCs and allows straightforward identification of prophase,

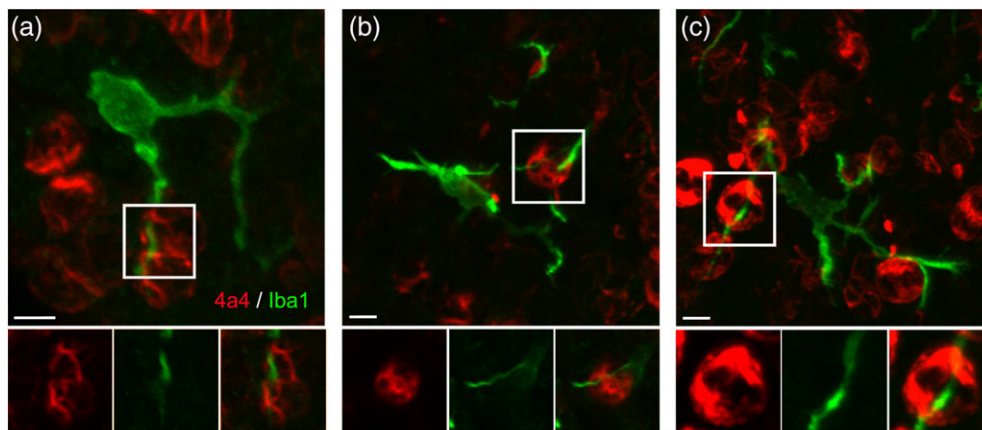


FIGURE 5 The processes of some periventricular microglia are very closely affiliated with NPC soma and appeared to course through the soma of 4A4⁺ dividing NPCs. Panels a, b, and c show the projected images of periventricular microglia in the E19 rat. Insets below highlight processes from these cells that extended to the ventricle and appeared to course through the soma of mitotic NPCs. We interpret these images as microglial processes that course through grooves or channels in the outer membrane of the mitotic NPCs. Scale bars = 5 μm [Color figure can be viewed at wileyonlinelibrary.com]

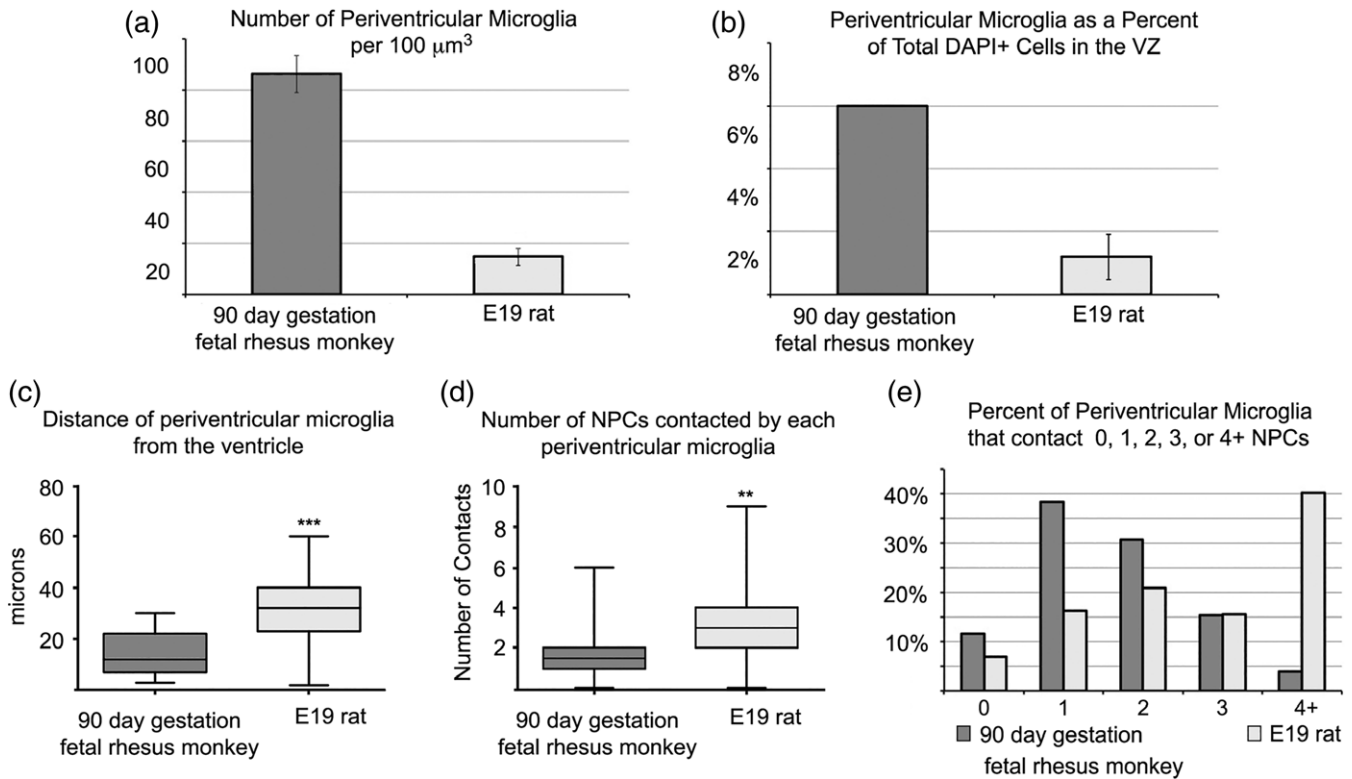


FIGURE 6 Comparison of periventricular microglia in the 90 days gestation fetal rhesus monkey and E19 rat. (a) The number of periventricular microglia is higher in the 90 days gestation fetal rhesus monkey compared to the E19 rat ($p < .01, **$). (b) The proportion of microglia in comparison to the total number of DAPI⁺ cells is higher in the periventricular zone of the fetal monkey. (c) Periventricular microglia were positioned significantly closer to the ventricle in 90 days gestation fetal rhesus monkey compared to E19 rat ($p < .0001, ***$). (d) Periventricular microglia in the E19 rat contacted more NPCs than in the fetal rhesus monkey ($p < .01, **$). (e) Periventricular microglia in the E19 rat were more likely to contact more than one NPC. E19 rat and 90 days gestation rhesus monkey represent the same stage of cortical neurogenesis. Due to different NPC dynamics (Martinez-Cerdeño et al., 2012), fewer NPCs divide at the ventricle at this stage of development in the fetal rhesus monkey, the VZ is significantly thinner, and microglia may be positioned closer to the ventricle in the rhesus monkey as a result

metaphase, anaphase, and telophase stages of mitosis (Weissman et al., 2003); 4A4 labels the soma of most mitotic precursor cells, including all mitotic radial glial cells in the rat and rhesus monkey VZ (Cunningham et al., 2013a; Noctor et al., 2002); and 4A4 labels the pial process of M-phase NPCs (Cunningham et al., 2013a; Noctor et al., 2002; Weissman et al., 2003).

4.1 | Periventricular microglia in rat and rhesus monkey

Rat and rhesus monkey periventricular microglia shared principal features. The cells were located in the VZ near the ventricle, possessed somata that were positioned superficial to mitotic NPCs undergoing division at the surface of the ventricle, and extended processes that contacted dividing NPCs. In both species the soma of periventricular microglia was $\sim 10 \mu\text{m}$ in diameter, the cells extended three or four main processes from the soma, and the processes occupied a territory of $\sim 60 \mu\text{m}^3$. However, there were several notable differences between rat and rhesus monkey. The density of microglia was significantly greater in fetal rhesus monkey, as we have previously reported (Barger et al., 2018). Periventricular microglia had processes that were more ramified and extended voluminous membranes that contacted and enveloped multiple neighboring cells in fetal rhesus monkey, but

not in the rat. These differences may reflect functional differences between the species, but may also correlate with the higher number of NPCs that populate the proliferative zones of the rhesus monkey (Martinez-Cerdeño et al., 2012). We also noted that periventricular microglia were positioned closer to the ventricle in the rhesus monkey. The difference in the distance of periventricular microglial somata from the ventricle in rat and rhesus monkey may result from interactions between microglia and NPCs. While our data were drawn from species at the same stage of cortical neurogenesis, there are significant differences in cellular dynamics and thickness of the VZ and SVZ between rat and rhesus monkey. The thickness of the VZ is a function of the number of precursor cells that proliferate in the VZ (Takahashi, Nowakowski, & Caviness, 1995), and this measure reaches a maximum before the appearance of the SVZ (Bayer & Altman, 1991; Martinez-Cerdeño et al., 2012). In rhesus monkeys the majority of neurogenic divisions shift away from the ventricle to the SVZ at an earlier stage of cortical neurogenesis compared to rat (Martinez-Cerdeño et al., 2012; Smart et al., 2002). As a result, the VZ is thinner in monkeys during production of neurons destined for the upper cortical layers than it is in the rat at the same stage of neurogenesis. The data indicate that, as the VZ becomes thinner periventricular microglia move closer to the ventricle, and suggest that microglial cell position

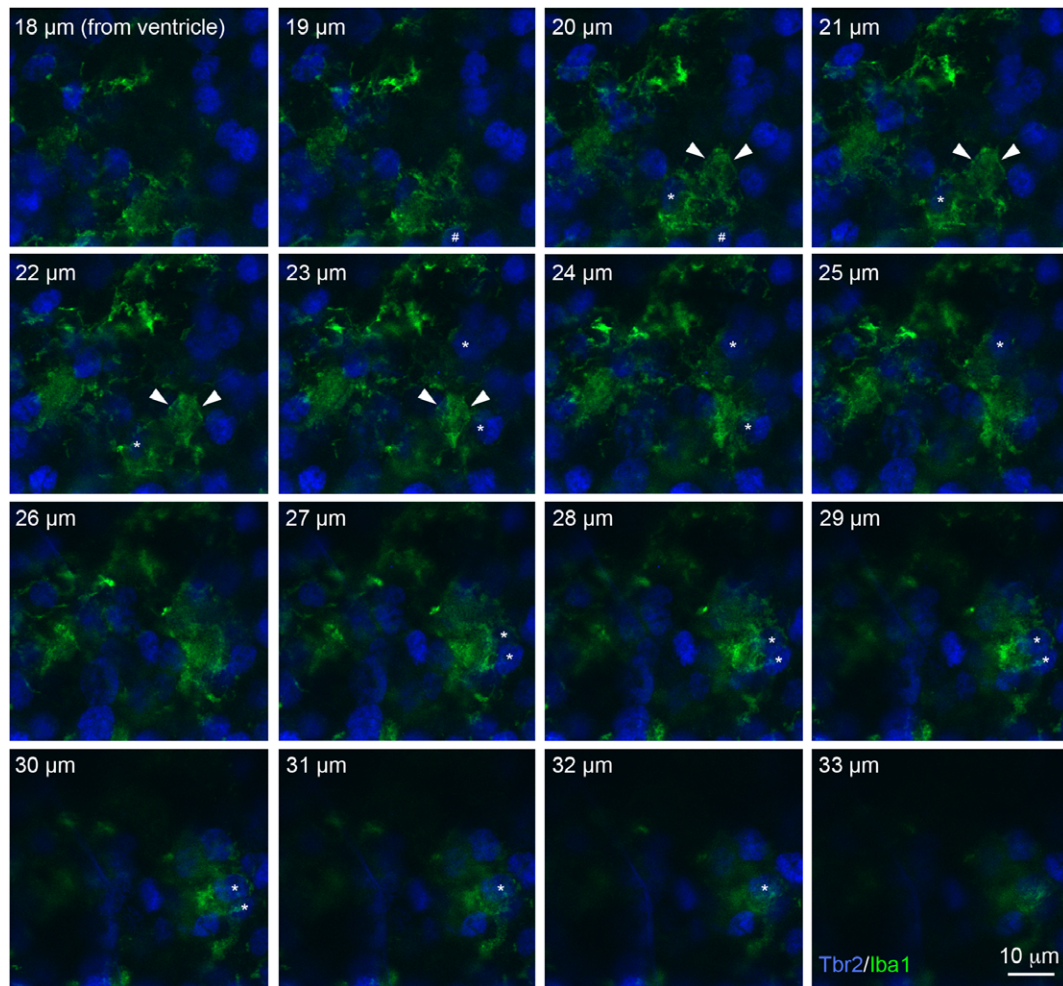


FIGURE 7 Periventricular microglia (Iba1, green) in 90 days gestation fetal rhesus monkey had complex morphology and some of these cells extended large membranous sheets that contacted and enveloped neighboring Tbr2⁺ NPCs. The soma of this periventricular microglial cell was positioned 20 μm from the surface of the lateral ventricle and is indicated in optical planes 20–23 μm with white arrowheads. The cell extended a phagocytic cup that encircled a Tbr2⁺ NPC (hashtag) in optical planes 18–20 μm . Five Tbr2⁺ NPCs (blue) that were enveloped by the membranous extension from this periventricular microglial cell (asterisks) are visible in the optical planes at 20–22 μm (1 cell), 22–25 μm (2 cells) and 27–32 μm (2 cells). Scale bar = 10 μm . The Z-stack can be viewed as a QuickTime movie in Supporting Information Movie 2 [Color figure can be viewed at wileyonlinelibrary.com]

in the proliferative zones is responsive to the dynamic behaviors of the NPC population. We noted that periventricular microglia contacted more NPCs in the E19 rat than in the 90 days gestation fetal rhesus monkey. However, this may also be a function of developmental dynamics in the rhesus monkey as well since the majority of NPC divisions shift to the SVZ by 90 days gestation, and fewer divisions occur at the ventricle (Martinez-Cerdeño et al., 2012; Smart et al., 2002). A developmental study across gestation in both species would shed light on the position, persistence, and function of periventricular microglia in the developing mammalian neocortex.

4.2 | Functional significance of contacts between periventricular microglia and NPCs

NPCs dividing at the surface of the ventricle are multipotent precursor cells. Lineage studies and immunohistochemical analyses we have performed in rat show that during late stages of prenatal cortical development NPCs dividing at the ventricle yield radial glial cells,

translocating radial glial cells, Tbr2⁺ intermediate progenitor cells, neurons, and astroglia (Martinez-Cerdeño et al., 2012; Noctor et al., 2004; Noctor et al., 2008; Noctor, Flint, Weissman, Dammerman, & Kriegstein, 2001). Our work in the fetal rhesus monkey indicates that NPC surface divisions produce translocating radial glial cells, Tbr2⁺ intermediate progenitor cells, and some self-renewed radial glial cells. In addition, we have found that Tbr2⁺ NPCs divide at the surface of the ventricle during late stages of neurogenesis (Barger et al., 2018; Cunningham et al., 2013a). Thus, key cell fate decisions that impact cellular composition of the cerebral cortex occur at the ventricle during this stage of development in rat and monkey. Our data show that individual periventricular microglia contact the soma and pial fiber of multiple mitotic NPCs, and also make multiple contacts with the same NPC, thus indicating that periventricular microglia have the potential to contribute to NPC proliferation and cell division outcomes. Consistent with this idea, recent evidence suggests that cell types in contact with radial glial cells, such as Tbr2⁺ intermediate progenitor cells, impact radial glial cell function via cell–cell signaling (Hatakeyama

et al., 2014; Kawaguchi et al., 2008; Yoon et al., 2008). Microglial cells are known to release multiple signals, including cytokines, chemokines, and growth factors, that impact function of receptive cells (Wolf et al., 2017). How microglia impact the function of NPCs in the fetal cerebral cortex remains to be determined.

4.3 | Health implications

Microglia are the innate immune cells of the central nervous system (Hagberg, Gressens, & Mallard, 2012; Wolf et al., 2017), and are competent to respond to external cues in the prenatal brain. We previously showed that microglia in the embryonic rat brain respond to maternal exposure to immunogenic agents such as lipopolysaccharide (Cunningham et al., 2013b). Data from the past decade support that maternal inflammatory immune responses impact health outcomes for the developing fetus (Deverman & Patterson, 2009; Hagberg et al., 2012; Mattei et al., 2017; Meyer, 2013; Meyer, Feldon, & Fatemi, 2009; Salter & Stevens, 2017; Wolf et al., 2017). In addition to contacting NPCs, periventricular microglia in the prenatal brain also extend processes that contact blood vessels and the ventricular surface where they may have access to cerebrospinal fluid in the lateral ventricle. In this way, the morphological features of microglia could make them an exceptionally responsive sentinel and conduit for intrinsic as well as extrinsic signaling in the prenatal cortex. Our data that shows periventricular microglia make extensive contact with mitotic NPCs—precursor cells in the very act of forming new neural and glial cells for the developing cerebrum—demonstrate direct neuroimmune interactions in the fetal proliferative zones. This suggests intercellular communication between these cell types and provides a neuroimmune mechanism for regulating NPC function under normal and aberrant developmental conditions. Our current findings demonstrate that periventricular microglia contribute to the complex environment that surrounds mitotic NPCs in the fetal brain. The most pertinent implication of these findings is that altering the function of fetal microglia by intrinsic signaling or by exposure to developmental pathogens may impact NPC function. Altering these functions could change the timing and trajectory of normal development and increase susceptibility for altered neurodevelopmental outcomes as well as pathology across the lifespan.

ACKNOWLEDGMENTS

These studies were supported by National Institutes of Health grant MH101188 to SCN; the MIND Institute (IDDR; U54 HD079125); the University of California, Davis Department of Psychiatry and Behavioral Sciences, the NHLBI Center for Fetal Monkey Gene Transfer for Heart, Lung, and Blood Diseases (NIH grant #HL085794 to AFT), and the California National Primate Research Center base operating grant (#OD011107).

ORCID

Stephen C. Noctor  <https://orcid.org/0000-0001-5236-4525>

Verónica Martínez-Cerdeño  <https://orcid.org/0000-0002-9613-3603>

REFERENCES

- Alliot, F., Godin, I., & Pessac, B. (1999). Microglia derive from progenitors, originating from the yolk sac, and which proliferate in the brain. *Brain Research. Developmental Brain Research*, 117(2), 145–152.
- Andjelkovic, A. V., Nikolic, B., Pachter, J. S., & Zecevic, N. (1998). Macrophages/microglial cells in human central nervous system during development: An immunohistochemical study. *Brain Research*, 814(1–2), 13–25.
- Arno, B., Grassivaro, F., Rossi, C., Bergamaschi, A., Castiglioni, V., Furlan, R., ... Muzio, L. (2014). Neural progenitor cells orchestrate microglia migration and positioning into the developing cortex. *Nature Communications*, 5, 5611. <https://doi.org/10.1038/ncomms6611>
- Barger, N., Keiter, J. A., Kreutz, A., Krishnamurthy, A., Weidenthaler, C., Martínez-Cerdeño, V., ... Noctor, S. C. (2018). Microglia: An intrinsic component of the proliferative zones in the fetal rhesus monkey (*Macaca mulatta*) cerebral cortex. *Cerebral Cortex*. <https://doi.org/10.1093/cercor/bhy145>
- Bayer, S. A., & Altman, J. (1991). *Neocortical Development*. New York: Raven Press.
- Cunningham, C. L., Martínez-Cerdeño, V., & Noctor, S. C. (2013a). Diversity of neural precursor cell types in the prenatal macaque cerebral cortex exists largely within the Astroglial cell lineage. *PLoS One*, 8(5), e63848. <https://doi.org/10.1371/journal.pone.0063848>
- Cunningham, C. L., Martínez-Cerdeño, V., & Noctor, S. C. (2013b). Microglia regulate the number of neural precursor cells in the developing cerebral cortex. *The Journal of Neuroscience*, 33(10), 4216–4233.
- Deverman, B. E., & Patterson, P. H. (2009). Cytokines and CNS development. *Neuron*, 64(1), 61–78. <https://doi.org/10.1016/j.neuron.2009.09.002>
- Ginhoux, F., Greter, M., Leboeuf, M., Nandi, S., See, P., Gokhan, S., ... Merad, M. (2010). Fate mapping analysis reveals that adult microglia derive from primitive macrophages. *Science*, 330(6005), 841–845. <https://doi.org/10.1126/science.1194637>
- Hagberg, H., Gressens, P., & Mallard, C. (2012). Inflammation during fetal and neonatal life: Implications for neurologic and neuropsychiatric disease in children and adults. *Annals of Neurology*, 71(4), 444–457. <https://doi.org/10.1002/ana.22620>
- Hatakeyama, J., Wakamatsu, Y., Nagafuchi, A., Kageyama, R., Shigemoto, R., & Shimamura, K. (2014). Cadherin-based adhesions in the apical ectoderm are required for active notch signaling to control neurogenesis in vertebrates. *Development*, 141(8), 1671–1682. <https://doi.org/10.1242/dev.102988>
- His, W. (1889). Die Neuroblasten und deren Entstehung im embryonalen Mark. *Abh. Kgl. sachs. Ges. Wissensch. math. phys. Kl.*, 15, 311–372.
- Imai, Y., Iбата, I., Ito, D., Ohsawa, K., & Kohsaka, S. (1996). A novel gene *iba1* in the major histocompatibility complex class III region encoding an EF hand protein expressed in a monocytic lineage. *Biochemical and Biophysical Research Communications*, 224(3), 855–862. <https://doi.org/10.1006/bbrc.1996.1112>
- Kamei, Y., Inagaki, N., Nishizawa, M., Tsutsumi, O., Taketani, Y., & Inagaki, M. (1998). Visualization of mitotic radial glial lineage cells in the developing rat brain by Cdc2 kinase-phosphorylated vimentin. *Glia*, 23(3), 191–199.
- Kawaguchi, A., Ikawa, T., Kasukawa, T., Ueda, H. R., Kurimoto, K., Saitou, M., & Matsuzaki, F. (2008). Single-cell gene profiling defines differential progenitor subclasses in mammalian neurogenesis. *Development*, 135(18), 3113–3124. <https://doi.org/10.1242/dev.022616>
- Martínez-Cerdeño, V., Cunningham, C. L., Camacho, J., Antczak, J. L., Prakash, A. N., Cziep, M. E., ... Noctor, S. C. (2012). Comparative analysis of the subventricular zone in rat, ferret and macaque: Evidence for an outer subventricular zone in rodents. *PLoS One*, 7(1), e30178. <https://doi.org/10.1371/journal.pone.0030178>
- Mattei, D., Ivanov, A., Ferrai, C., Jordan, P., Guneykaya, D., Buonfiglioli, A., ... Wolf, S. A. (2017). Maternal immune activation results in complex microglial transcriptome signature in the adult offspring that is reversed by minocycline treatment. *Translational Psychiatry*, 7(5), e1120. <https://doi.org/10.1038/tp.2017.80>
- Meyer, U. (2013). Developmental neuroinflammation and schizophrenia. *Progress in Neuro-Psychopharmacology & Biological Psychiatry*, 42, 20–34. <https://doi.org/10.1016/j.pnpbp.2011.11.003>

- Meyer, U., Feldon, J., & Fatemi, S. H. (2009). In-vivo rodent models for the experimental investigation of prenatal immune activation effects in neurodevelopmental brain disorders. *Neuroscience and Biobehavioral Reviews*, 33(7), 1061–1079. <https://doi.org/10.1016/j.neubiorev.2009.05.001>
- Noctor, S. C., Flint, A. C., Weissman, T. A., Dammerman, R. S., & Kriegstein, A. R. (2001). Neurons derived from radial glial cells establish radial units in neocortex. *Nature*, 409, 714–720.
- Noctor, S. C., Flint, A. C., Weissman, T. A., Wong, W. S., Clinton, B. K., & Kriegstein, A. R. (2002). Dividing precursor cells of the embryonic cortical ventricular zone have morphological and molecular characteristics of radial glia. *The Journal of Neuroscience*, 22(8), 3161–3173.
- Noctor, S. C., Martínez-Cerdeño, V., Ivic, L., & Kriegstein, A. R. (2004). Cortical neurons arise in symmetric and asymmetric division zones and migrate through specific phases. *Nature Neuroscience*, 7(2), 136–144.
- Noctor, S. C., Martínez-Cerdeño, V., & Kriegstein, A. R. (2008). Distinct behaviors of neural stem and progenitor cells underlie cortical neurogenesis. *The Journal of Comparative Neurology*, 508(1), 28–44.
- Paolicelli, R. C., Bolasco, G., Pagani, F., Maggi, L., Scianni, M., Panzanelli, P., ... Gross, C. T. (2011). Synaptic pruning by microglia is necessary for normal brain development. *Science*, 333(6048), 1456–1458. <https://doi.org/10.1126/science.1202529>
- Rakic, P. (1974). Neurons in rhesus monkey visual cortex: Systematic relation between time of origin and eventual disposition. *Science*, 183(123), 425–427.
- Salter, M. W., & Stevens, B. (2017). Microglia emerge as central players in brain disease. *Nature Medicine*, 23(9), 1018–1027. <https://doi.org/10.1038/nm.4397>
- Schafer, D. P., Lehrman, E. K., Kautzman, A. G., Koyama, R., Mardinly, A. R., Yamasaki, R., ... Stevens, B. (2012). Microglia sculpt postnatal neural circuits in an activity and complement-dependent manner. *Neuron*, 74(4), 691–705. <https://doi.org/10.1016/j.neuron.2012.03.026>
- Smart, I. H., Dehay, C., Giroud, P., Berland, M., & Kennedy, H. (2002). Unique morphological features of the proliferative zones and postmitotic compartments of the neural epithelium giving rise to striate and extrastriate cortex in the monkey. *Cerebral Cortex*, 12(1), 37–53.
- Squarzone, P., Oller, G., Hoeffel, G., Pont-Lezica, L., Rostaing, P., Low, D., ... Garel, S. (2014). Microglia modulate wiring of the embryonic forebrain. *Cell Reports*, 8(5), 1271–1279. <https://doi.org/10.1016/j.celrep.2014.07.042>
- Swinnen, N., Smolders, S., Avila, A., Notelaers, K., Paesen, R., Ameloot, M., ... Rigo, J. M. (2013). Complex invasion pattern of the cerebral cortex by microglial cells during development of the mouse embryo. *Glia*, 61(2), 150–163. <https://doi.org/10.1002/glia.22421>
- Takahashi, T., Nowakowski, R. S., & Caviness, V. S., Jr. (1995). The cell cycle of the pseudostratified ventricular epithelium of the embryonic murine cerebral wall. *Journal of Neuroscience*, 15(9), 6046–6057.
- Tang, X., Falls, D. L., Li, X., Lane, T., & Luskin, M. B. (2007). Antigen-retrieval procedure for bromodeoxyuridine immunolabeling with concurrent labeling of nuclear DNA and antigens damaged by HCl pretreatment. *The Journal of Neuroscience*, 27(22), 5837–5844. <https://doi.org/10.1523/JNEUROSCI.5048-06.2007>
- Tarantal, A. F. (2005). Ultrasound imaging in rhesus (*Macaca mulatta*) and long-tailed (*Macaca fascicularis*) macaques: Reproductive and research applications. *The Laboratory Primate* (pp. 317–351): Elsevier Academic Press.
- Tarantal, A. F., Salamat, M. S., Britt, W. J., Luciw, P. A., Hendrickx, A. G., & Barry, P. A. (1998). Neuropathogenesis induced by rhesus cytomegalovirus in fetal rhesus monkeys (*Macaca mulatta*). *The Journal of Infectious Diseases*, 177(2), 446–450.
- Ueno, M., Fujita, Y., Tanaka, T., Nakamura, Y., Kikuta, J., Ishii, M., & Yamashita, T. (2013). Layer V cortical neurons require microglial support for survival during postnatal development. *Nature Neuroscience*, 16(5), 543–551. <https://doi.org/10.1038/nn.3358>
- Verney, C., Monier, A., Fallet-Bianco, C., & Gressens, P. (2010). Early microglial colonization of the human forebrain and possible involvement in periventricular white-matter injury of preterm infants. *Journal of Anatomy*, 217(4), 436–448. <https://doi.org/10.1111/j.1469-7580.2010.01245.x>
- Weissman, T., Noctor, S. C., Clinton, B. K., Honig, L. S., & Kriegstein, A. R. (2003). Neurogenic radial glial cells in reptile, rodent and human: From mitosis to migration. *Cerebral Cortex*, 13(6), 550–559.
- Wolf, S. A., Boddeke, H. W., & Kettenmann, H. (2017). Microglia in physiology and disease. *Annual Review of Physiology*, 79, 619–643. <https://doi.org/10.1146/annurev-physiol-022516-034406>
- Yoon, K. J., Koo, B. K., Im, S. K., Jeong, H. W., Ghim, J., Kwon, M. C., ... Kong, Y. Y. (2008). Mind bomb 1-expressing intermediate progenitors generate notch signaling to maintain radial glial cells. *Neuron*, 58(4), 519–531.

SUPPORTING INFORMATION

Additional supporting information may be found online in the Supporting Information section at the end of the article.

How to cite this article: Noctor SC, Penna E, Shepherd H, et al. Periventricular microglial cells interact with dividing precursor cells in the nonhuman primate and rodent prenatal cerebral cortex. *J Comp Neurol*. 2019;1–12. <https://doi.org/10.1002/cne.24604>